

SYNTHESIS, CHARACTERIZATION, DIELECTRIC AND THERMOELECTRIC PROPERTIES OF CALCIUM DOPED MAGNESIUM TITANATE $\text{Mg}_{(1-x)}\text{Ca}_x\text{TiO}_3$ (x=0.1, 0.3 & 0.5) CERAMICS

V. S. SAMYUKTHA^{a*}, T. SUBBARAO^b, R. P. SUVARNA^a, A. G. KUMAR^c

^a*Department of Physics, Jawaharlal Nehru Technological University, Anantapuramu, Andhra Pradesh, India*

^b*Materials Research Lab, Department of Physics, Sri KrishnaDevaraya University, Anantapuramu, Andhra Pradesh, India.*

^c*Department of Physics, Mallareddy Engineering College, Hyderabad, Telangana, India.*

The Calcium Doped Magnesium Titanate ceramic materials of different compositions were synthesized by conventional Solid-state diffusion method. The results of XRD and microstructure analysis showed that the specimens had crystalline, homogenous and dense structures. The dielectric constant from room temperature to 350°C was calculated using HIOKI 3532-50 LCR HiTESTER in the frequency range of 1KHz-1MHz. In the present investigation the dielectric response of Calcium doped Magnesium titanate was studied. It showed that the dielectric constant and dielectric loss were increased with temperature and decreased with frequency and also observed the enhancement of dielectric constant with the addition of small amount of Calcium to the Magnesium Titanate ceramics. The a.c. conductivity of the specimens were measured and thermoelectric properties were also studied.

(Received October 31, 2016; Accepted February 3, 2017)

Keywords: Solid State diffusion method, Dielectric Constant, a.c. conductivity, XRD, SEM

1. Introduction

In the recent decades ceramic materials have a wide range of importance in various fields of communication systems, power transmission, computers, consumer and military electronics depending upon their suitability. The ceramic materials industry is the source of many other industries for instance, glass ceramics are used in architectural, electronic and electrical industries, Abrasives are used in machine-tool and automobile industries, and many more. Newly designed devices essentially include these materials because of their novel chemical, electrical, optical, dielectric, mechanical, thermal and structural properties.

Magnesium Titanate ceramics play an important role in microwave technologies such as global positioning system operating at microwave frequencies, resonators, filters, antennas for communication system and multilayer capacitors [1-4]. It is a multifaceted material of low dielectric loss with high quality factor (Q above 20000 at 8GHz) and intermediate dielectric constant ($\epsilon_r=17$) [5]. An MgTiO_3 ceramic exhibits ilmenite structure with Hexagonal crystal system and belongs to R-3 group [6]. Dielectric resonators, used in microwave frequency have been widely investigated due to the fast growth of satellite and mobile communication systems. MgTiO_3 (MT) is reported to exhibit good dielectric properties of $\epsilon_r \sim 17$, $Q \times f \sim 160,000$ at 7GHz and $\tau_f \sim -50$ ppm/°C.

In the present work, the calcium doped magnesium titanate ceramic materials of different compositions such as $\text{Mg}_{(1-x)}\text{Ca}_x\text{TiO}_3$ (x=0.1,0.3&0.5) were synthesized by conventional Solid State diffusion method and the phase, crystallite size, microstructure, dielectric properties and thermoelectrical properties were investigated.

* Corresponding author: vsharonsamyuktha@gmail.com

2. Experimental procedure

High purity materials such as MgO (99.6% purity, Sigma Aldrich), TiO₂ (99.4% purity, Sigma Aldrich) and CaO (99.6% purity, Sigma Aldrich) were used as starting materials. These materials were taken according to the composition and mixed uniformly. The mixed powder was milled for 12h in a Ball Mill (Retsch PM 200). These mixtures were dried moreover taken in alumina crucibles calcined at 1150-1200⁰C for 36h in air in a programmable furnace. These calcined powders were again milled for 10h. Then the powders were pressed into pellets by adding PVA binder and by applying pressure of 8 ton using Hydraulic press. These readily formed pellets were sintered at a temperature of 1250-1300⁰C for 4h in the furnace with a heating rate of 10⁰C/min and then cooled to room temperature.

The lattice parameters and crystalline phases of the sintered samples were identified by X-Ray diffractometer (Rigaku), using CuK α radiation. Microstructural analysis of the sintered samples was performed by SEM (Hitachi: S-4700) and Energy Dispersive X-Ray Spectroscopy (EDAX). The dielectric constant, dielectric loss and AC conductivity were measured by LCR meter HIOKI 3252-50 in the frequency range 1KHz to 1MHz. The dielectric constant was measured by [7]

$$\epsilon_r = \frac{C * d}{\epsilon_0 * A} \quad (1)$$

where C is capacitance of the pellet, d is thickness of the pellet; A is the area of the cross section of the pellet and ϵ_0 is the permittivity of free space. The AC conductivity of the samples was estimated from dielectric parameters. The AC conductivity (σ_{ac}) was calculated using the relation

$$\sigma_{ac} = \epsilon_0 \epsilon_r \omega \tan \delta \quad (2)$$

where ϵ_0 is the permittivity of the free space, ϵ_r = dielectric constant, $\omega = 2\pi f$ is the angular frequency and $\tan \delta$ is the loss tangent. The thermoelectric properties were also thoroughly studied.

3. Results and discussion

3.1 XRD Analysis

The crystalline structure of Mg_(1-x)Ca_xTiO₃ (x=0.1,0.3&0.5) ceramic samples was evaluated by XRD analysis at room temperature, using Rigaku X-Ray Powder Diffract Meter (Japan) was shown in fig.1.

Hexagonal crystalline structure having single reflection peaks with the exception of few additional phases corresponding to the presence of CaTiO₃ (CT) and MgTi₂O₅ exhibited by the samples was observed. The MgTi₂O₅ requires a high sintering temperature of 1450⁰C. So secondary phase MgTi₂O₅ was formed as intermediate phase and difficult to eliminate from sample, prepared by conventional solid state route [8]. Since the ionic size of Calcium was greater than Magnesium, the Calcium Titanate was formed as an additional phase. The intensity of the diffraction pattern depends on structure factor would show the XRD data of present sample, and the average crystallite size (D_p) was obtained using Scherer formula [9]

$$D_p = k\lambda/\beta \cos \theta \quad (3)$$

where k is a constant and is equal to 0.9, θ is diffraction angle, $\lambda = 0.154056$ nm (CuK α) and β is full width half maxima. The dislocation density was calculated by the formula $\rho = D^{-2}$ where D is average crystalline size.

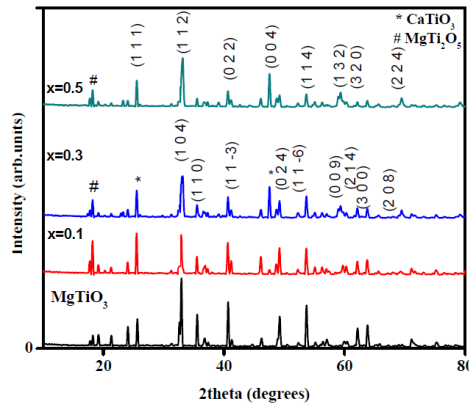


Fig.1. XRD pattern of $Mg_{(1-x)}Ca_xTiO_3$ ceramic samples.

The average crystallite size, dislocation density and strain were also calculated and tabulated. The strain values were positive indicate the tensile strain for all the samples.

Table 1. displays the values of average crystallite size, dislocation density and Strain for the $Mg_{(1-x)}Ca_xTiO_3$ ($x=0.1, 0.3$ & 0.5) samples.

S.No.	Compound name	Average Crystallite size (nm)	Dislocation Density m^{-2}	Strain
1	$Mg_{0.9}Ca_{0.1}TiO_3$	72.83	1.885×10^{14}	0.0881
2	$Mg_{0.7}Ca_{0.3}TiO_3$	70.87	1.991×10^{14}	0.0871
3	$Mg_{0.5}Ca_{0.5}TiO_3$	61.13	2.676×10^{14}	0.1578

The maximum intensity peak was observed at 2θ of 32.9° for the plane (1 0 4) for $Mg_{0.9}Ca_{0.1}TiO_3$ ceramic sample where it exhibited hexagonal structure and the peaks were indexed (ICDD #06-0494) and the lattice parameters were identified as $a=b=5.057A^\circ$ and $c=13.913A^\circ$ and for $Mg_{0.7}Ca_{0.3}TiO_3$ ceramic sample the maximum reflection peak also occurred at (1 0 4) and $a=b=5.055A^\circ$ and $c=13.899A^\circ$ of Hexagonal structure. The compound $Mg_{0.5}Ca_{0.5}TiO_3$ exhibited orthorhombic structure (ICDD #22-0153) with lattice parameters given by $a=5.350 A^\circ$, $b=5.438 A^\circ$ and $c=7.696A^\circ$ respectively. This composition of ceramic material underwent a transition from Hexagonal structure to Orthorhombic which was due to heavy doping of calcium. The maximum intensity occurred at 2θ of 33.09° for the plane (1 1 2) which has good agreement with the literature.

3.2 SEM and EDAX results

The surface morphology was studied by Scanning Electron Microscopy. Fig.2 showed SEM images of $Mg_{(1-x)}Ca_xTiO_3$ ($x=0.1, 0.3$ & 0.5) which had been made at two different spots having 10,000X, 5000X and 2500X magnifications and in $5\mu m$, $10\mu m$ and $20\mu m$ range respectively. In the images the grains were mostly spherical in shape, containing homogeneous distribution with distinguished boundaries and with fewer pores had been observed. The SEM image of Fig.2 (a&b) included large grains, small grains and rod shaped grains. Few rod shaped grains were identified as $MgTi_2O_5$ which could not be eliminated in conventional solid state method. Similar grains were observed and analyzed to be $MgTi_2O_5$ by Huang et al. [1]. The large grains were identified as $MgTiO_3$ whereas the small grains were $MgTiO_3$ and $CaTiO_3$ coexisted [10].

The average grain size for ceramic samples $Mg_{(1-x)}Ca_xTiO_3$ ($x=0.1, 0.3$ & 0.5) was found to be nearly $5-7\mu m$ respectively, using the formula given in the equation (4) [11]. It was noticed that the secondary phase was reduced in $Mg_{0.5}Ca_{0.5}TiO_3$. The increase in grain size was due to sintering which enhanced the grain size. This high grain growth when compared with crystalline

size computed from XRD might be due to low elastic strain and thus high grain boundary creeping would occur.

EDAX was performed to determine the concentrations of elements such as Mg, Ca, Ti and O present in the ceramic samples. Fig.3 gives the At% and Wt% of various elements.

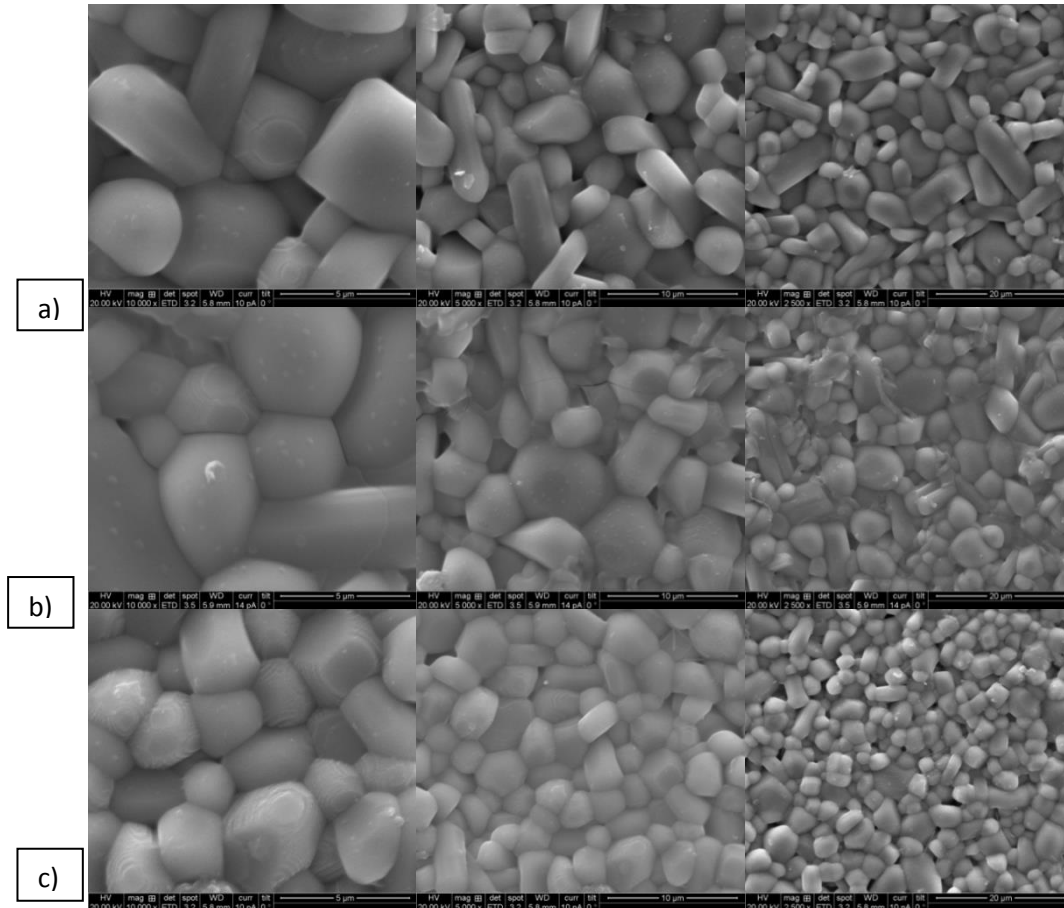


Fig.2 SEM images of a) $Mg_{0.9}Ca_{0.1}TiO_3$ b) $Mg_{0.7}Ca_{0.3}TiO_3$ and c) $Mg_{0.5}Ca_{0.5}TiO_3$ samples

$$\text{Average grain size} = \frac{1.5L}{MN} \quad (4)$$

Where L=the total test line length, M=the magnification, N=the total number of intercepts which the grain boundary makes with the line.

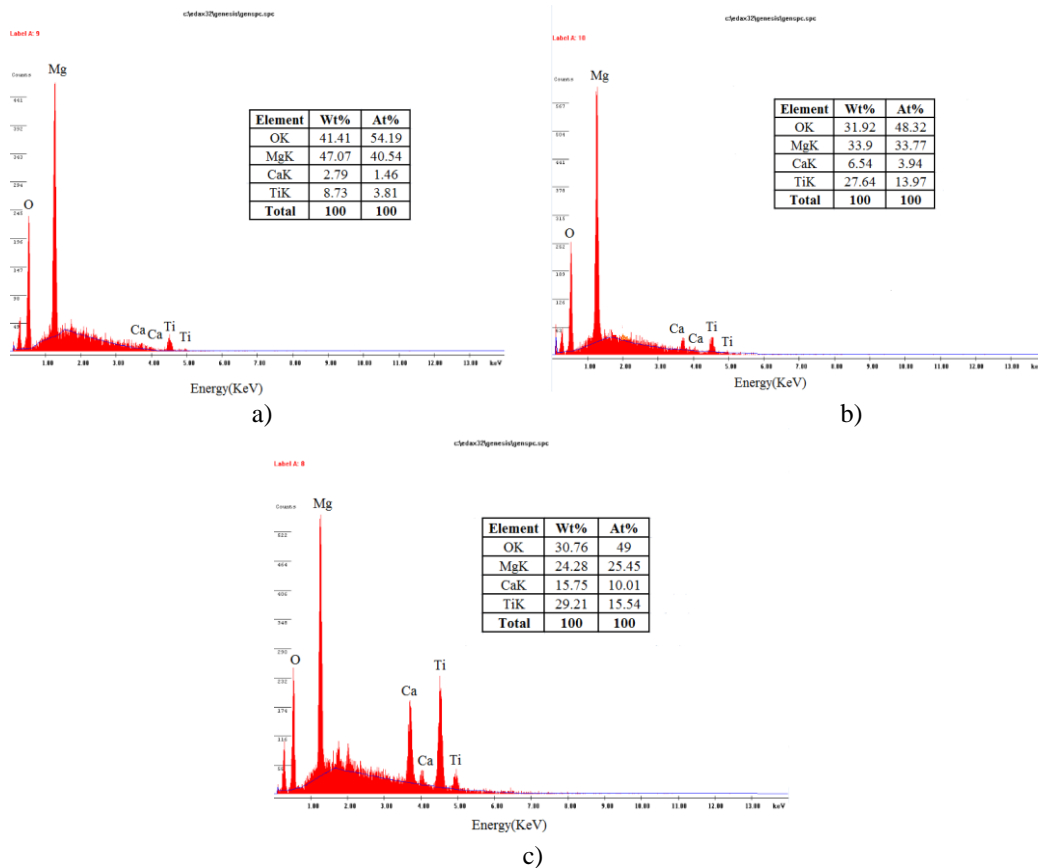


Fig.3 EDAX images of a) $Mg_{0.9}Ca_{0.1}TiO_3$ b) $Mg_{0.7}Ca_{0.3}TiO_3$ and c) $Mg_{0.5}Ca_{0.5}TiO_3$ samples

3.3 Dielectric properties

The dielectric properties of the sintered ceramic samples of Magnesium Calcium Titanate of various compositions were studied in the temperature range from room temperature to $350^{\circ}C$ of varying frequency of 1KHz to 1MHz. From fig 4. the variation of dielectric constant of ceramic samples $Mg_{(1-x)}Ca_xTiO_3$ ($x=0.1, 0.3$ & 0.5) with temperature at 1KHz was studied. The dielectric constant increased with increasing of x value and was almost stable with temperature but at high temperature its value increased. At low frequencies, the increase in dielectric constant with temperature was due to accumulation of charge at the grain boundary and at the interface of the electrode sample and the electrode which was called Space Charge Polarization [12]. As the frequency increased dielectric constant would decrease due to gradual diminishing of the space charge polarization, indicating the ionic contribution. The increase in dielectric constant was due to doping of Ca^{+2} ions, since $CaTiO_3$ ($\epsilon_r=170$) possess a much higher value than $MgTiO_3$.

The plot of Dielectric Loss with temperature at 1KHz frequency was shown in the fig.5 for the $Mg_{(1-x)}Ca_xTiO_3$ ($x=0.1, 0.3$ & 0.5) samples. At low frequency as temperature increased the dielectric loss increased which might be attributed to relaxation mechanism in the ceramic samples.

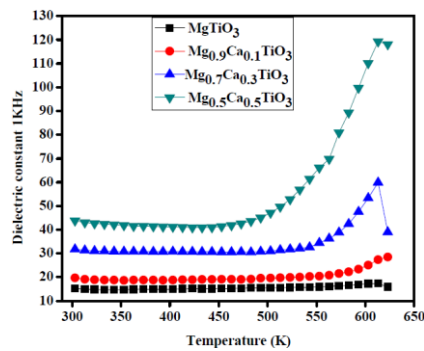


Fig. 4. Variation of Dielectric constant with temperature at 1KHz frequency for the ceramic samples $Mg_{(1-x)}Ca_xTiO_3$ ($x=0, 0.1, 0.3$ & 0.5)

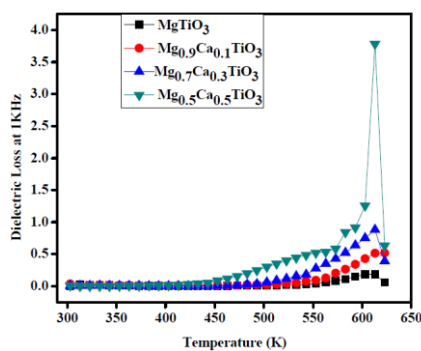


Fig. 5. Variation of Dielectric Loss with temperature at 1KHz frequency for the ceramic samples $Mg_{(1-x)}Ca_xTiO_3$ ($x=0, 0.1, 0.3$ & 0.5)

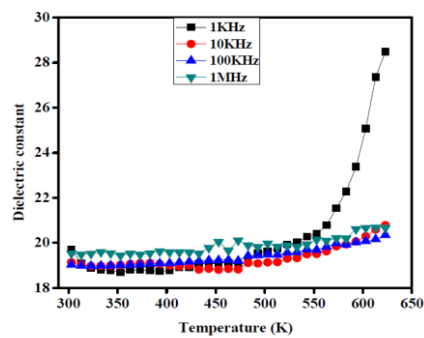


Fig. 6. Variation of Dielectric constant with temperature at different frequencies for the ceramic sample $Mg_{0.9}Ca_{0.1}TiO_3$

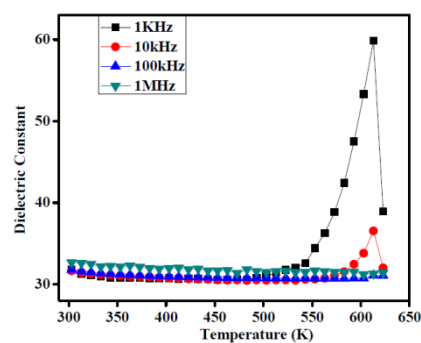


Fig. 7. Variation of Dielectric constant with temperature at different frequencies for the ceramic sample $Mg_{0.7}Ca_{0.3}TiO_3$

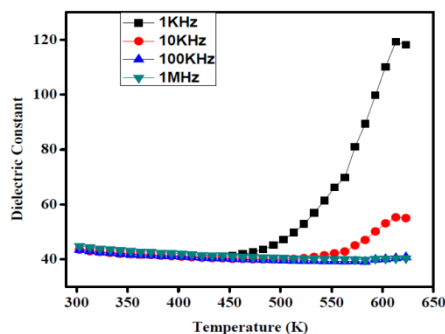


Fig. 8. Variation of Dielectric constant with temperature at different frequencies for the ceramic sample $Mg_{0.5}Ca_{0.5}TiO_3$

The dielectric constant variation with temperature of $Mg_{(1-x)}Ca_xTiO_3$ ($x=0.1, 0.3 \& 0.5$) at different frequencies ranging from 1KHz-1MHz with temperature were shown in the figs.6,7&8. It was observed that the dielectric constant was increased with temperature and decreased with frequency which might be due to the doping of Ca^{+2} ions, since $CaTiO_3$ ($\epsilon_r=170$) possessed a much higher value than $MgTiO_3$. The dielectric constant values obtained for $Mg_{0.9}Ca_{0.1}TiO_3$, $Mg_{0.7}Ca_{0.3}TiO_3$ and $Mg_{0.5}Ca_{0.5}TiO_3$ at 623k at 1MHz frequency were 21, 31.4 and 40.3 respectively.

In general the dielectric losses were due to distortional, dipolar conduction and interfacial, motion of charged ions. At higher frequencies, the dielectric loss observed in these samples was very less and almost stable which might be an extrinsic loss due to oxygen vacancies, grain size, secondary phases and densification. The variation of dielectric loss with temperature of ceramic samples $Mg_{(1-x)}Ca_xTiO_3$ ($x=0.1, 0.3 \& 0.5$) at different frequencies with temperature were apparently shown in the figures 9,10&11. The dielectric loss values obtained at 623K for a frequency of 1MHz for $Mg_{0.9}Ca_{0.1}TiO_3$, $Mg_{0.7}Ca_{0.3}TiO_3$ and $Mg_{0.5}Ca_{0.5}TiO_3$ were 0.04332, 0.00881 and 0.0127 respectively.

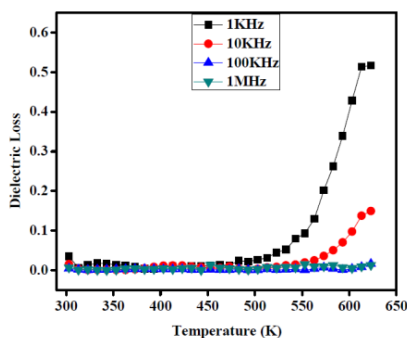


Fig. 9 Variation of Dielectric Loss with temperature at different frequencies for the ceramic sample $Mg_{0.9}Ca_{0.1}TiO_3$

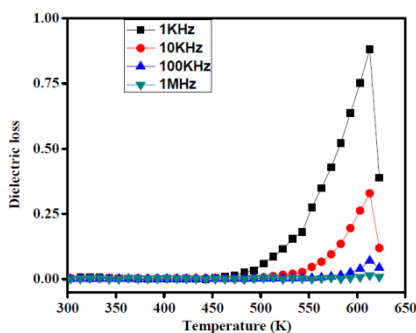


Fig. 10 Variation of Dielectric Loss with temperature at different frequencies for the ceramic sample $Mg_{0.7}Ca_{0.3}TiO_3$

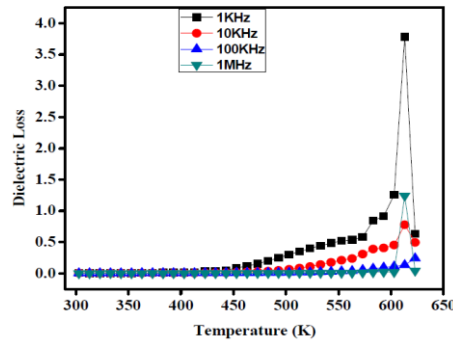


Fig. 11 Variation of Dielectric Loss with temperature at different frequencies for the ceramic sample $Mg_{0.5}Ca_{0.5}TiO_3$

The a.c. conductivity as a function of frequency at various temperatures for the samples $Mg_{(1-x)}Ca_xTiO_3$ ($x=0.1, 0.3$ & 0.5) were shown in the Figs. 12, 13 & 14. It was clear that the ac conductivity increased with increase in frequency of the applied a.c. field. As temperature increased, ac-conductivity also increased due to hopping of charge carriers and hence this could be given by the Arrhenius equation.

$$\sigma = \sigma_0 \exp\left(-\frac{E_a}{K_B T}\right) \quad (5)$$

Due to thermal activation process, the conductivity increased with increase of temperature which must be related to hopping of charge carriers which were bound in the localized states. Another reason could be attributed to the fact that the dopants can introduce defects which may lead to segregate at the grain boundaries due to diffusion process resulting from sintering and cooling processes.

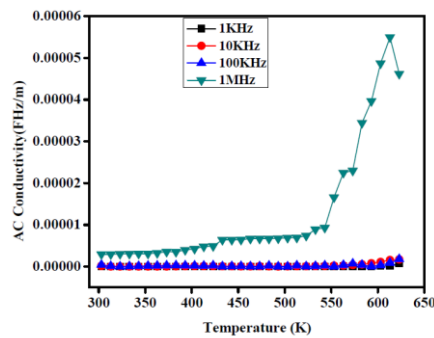


Fig. 12 Variation of a.c. conductivity as a function of temperature at different frequencies for the ceramic sample $Mg_{0.9}Ca_{0.1}TiO_3$

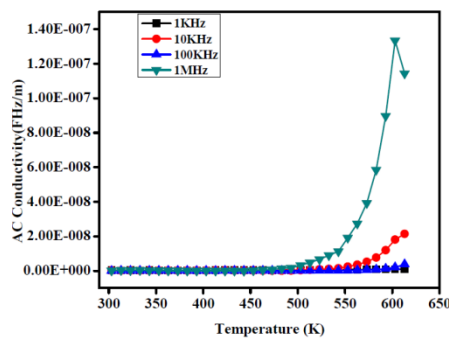


Fig. 13 Variation of a.c. conductivity as a function of temperature at different frequencies for the ceramic sample $Mg_{0.7}Ca_{0.3}TiO_3$

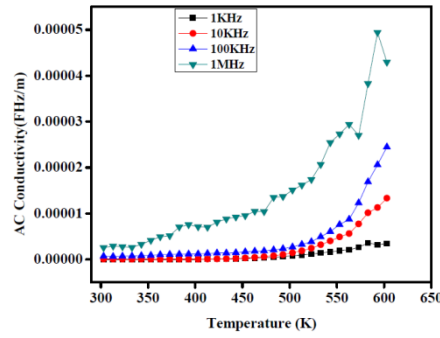


Fig. 14 Variation of a.c. conductivity as a function of temperature at different frequencies for the ceramic sample $Mg_{0.5}Ca_{0.5}TiO_3$

Figures 15, 17 & 19 showed the variation of Thermoemf (E) with temperature for $Mg_{(1-x)}Ca_xTiO_3$ ($x=0.1, 0.3$ & 0.5). Figures 16, 18 & 20 depicted the variation of Seebeck coefficient with temperature for $Mg_{(1-x)}Ca_xTiO_3$ ($x=0.1, 0.3$ & 0.5) ceramic samples and was positive which would reveal that holes were introduced. At high temperatures, Seebeck coefficient for all the samples slightly decreased and then increased with positive thermoelectric power (S). During the variation of temperature, the samples exhibited metallic nature. The carrier concentration (n) was calculated by using the following equation

$$n = \frac{N}{V} \exp\left(\frac{-Se}{K}\right) \quad (6)$$

Where $N=10^{22} \text{ cm}^{-3}$ (Density of the states), V is the volume of the sample, $K/e= 86.4 \mu\text{V/K}$ and S is Seebeck Coefficient.

The carrier concentration for $Mg_{0.9}Ca_{0.1}TiO_3$ was found to be $4.924 \times 10^{24}/\text{m}^{-3}$, for $Mg_{0.7}Ca_{0.3}TiO_3$ was $8.518 \times 10^{24}/\text{m}^{-3}$ and $Mg_{0.5}Ca_{0.5}TiO_3$ was $1.782 \times 10^{24}/\text{m}^{-3}$ respectively.

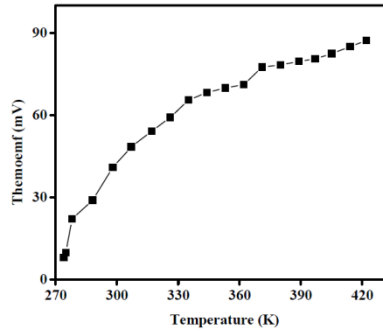


Fig. 15 Variation of Thermoemf with temperature for the ceramic sample $Mg_{0.9}Ca_{0.1}TiO_3$

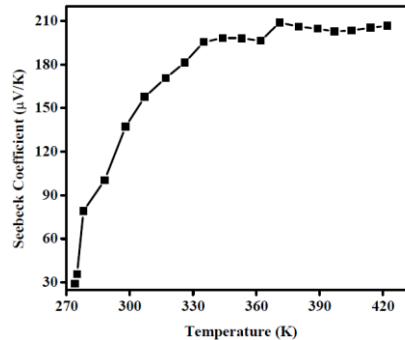


Fig. 16 Variation of Seebeck coefficient with temperature for the ceramic sample $Mg_{0.9}Ca_{0.1}TiO_3$

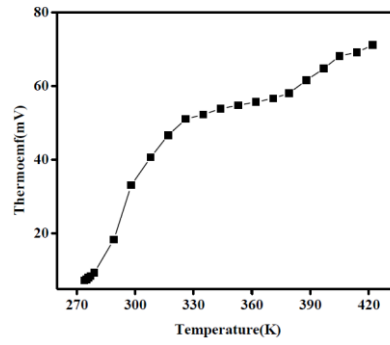


Fig. 17 Variation of Thermoemf with temperature for the ceramic sample $Mg_{0.7}Ca_{0.3}TiO_3$

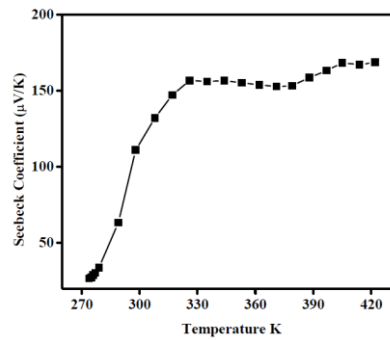


Fig. 18 Variation of Seebeck coefficient with temperature for the ceramic sample $Mg_{0.7}Ca_{0.3}TiO_3$

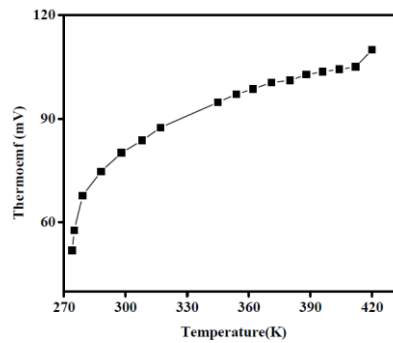


Fig. 19 Variation of Thermoemf with temperature for the ceramic sample $Mg_{0.5}Ca_{0.5}TiO_3$

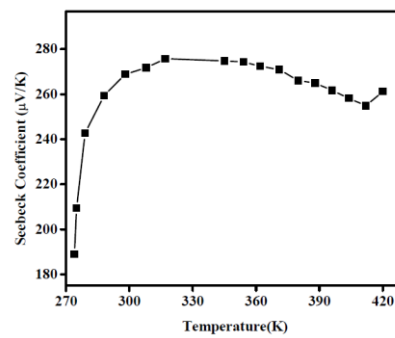


Fig. 20 Variation of Seebeck coefficient with temperature for the ceramic sample $Mg_{0.5}Ca_{0.5}TiO_3$

4. Conclusions

The XRD analysis showed no change in crystal structure of MgTiO_3 after doping with calcium for $\text{Mg}_{0.9}\text{Ca}_{0.1}\text{TiO}_3$ and $\text{Mg}_{0.7}\text{Ca}_{0.3}\text{TiO}_3$ and was of Hexagonal structure except for $\text{Mg}_{0.5}\text{Ca}_{0.5}\text{TiO}_3$ exhibits Orthorhombic structure. The SEM analysis unveiled the uniform distribution of grains with fewer pores. EDAX confirmed the presence of Mg, Ca, Ti and O elements. At the low frequencies, the dielectric constant increased with increase of temperature, whereas at high frequencies dielectric constant was almost stable and slightly increased at high temperature.

The dielectric loss was constant at high frequency. So these materials can be used for high frequency devices. $\text{Mg}_{(1-x)}\text{Ca}_x\text{TiO}_3$ ($x=0.1, 0.3$ & 0.5) ceramic materials are suitable for microwave device applications. As the frequency increased the magnitude of a.c. conductivity also increased for all samples. The Thermoelectric power also increased with temperature for all the samples.

References

- [1] C.L. Huang, et al., Mater. Res. Bull. **37**, 2483 (2002).
- [2] W.W.Cho, K.Kakimoto, H. Ohsato, Mater. Sci. Eng. B **121**,48 (2005).
- [3] R.Z. Chen, et al., Mater. Sci. Eng. B **99**,302 (2003).
- [4] C.C. Cheng, T.E. Hsieh, I.N. Lin, J. Eur.Ceram. Soc. **23**,2553 (2003).
- [5] Yuan- Fu Deng, Shi-Di Tang, Liang-Qiang Lao, Shu-Zhang Zhan, Inorganica Chimica Acta **363**,827 (2010).
- [6] T.Santhosh Kumar, D.Goswami, D. Pamu, Advanced Material Letters, VBRI Press.
- [7] V. Sharon Samyuktha, T.Subba Rao, R.Padma Suvarna, International Journal of Engineering Research and Technology, ISSN: 2278-0181, Vol. 5 Issue 05, May-2016.
- [8] S.Kucheiko, J.W.Choi, H.J.Kim, H.J. Jung, J.Am.Ceram.Soc.**79**,2739 (1996).
- [9] K. C. Babu Naidu, T.Sofi Sarmash, M. Maddaiah, A. Gurusampath Kumar, D.JhansiRani, V.Sharon Samyuktha, L. Obulapathi, T.Subbarao, Journal of Ovonic Research **11**(2), 79 (2015).
- [10] Yih-Chien Chen, Shin- Min Tsao, Chang-Shin Lin, Shun-Chung Wang, Yu-Hua Chien, Journal of Alloys and Compounds **471**,347 (2009).
- [11] M.Maddaiah, K.Chandra Babu Naidu, D.Jhansi Rani, T. Subbarao, Journal of Ovonic Research **11**(3), 99 (2015).
- [12] J Liqiang, S Xiaojun, X Baifu, W Baiqi, C Weimin, F Hongganga, J.Solid State Chem. **177**, 3375 (2004).